NRC Research Press

ARTICLE

Ligand influence on intramolecular cyclometalation in bis(phosphinimine) rare earth alkyl complexes

Kevin R.D. Johnson, Breanne L. Kamenz, and Paul G. Hayes

Can. J. Chem. Downloaded from www.nrcresearchpress.com by University of Lethbridge on 04/11/16
For personal use only.

Abstract: The synthesis and reactivity of two new bis(phosphinimine)carbazole ligands (PippN=PMe_2)$_2$DMC (H$\mathbf{L_A}$, **3**) and (PippN=$P(C_4H_8)$)$_2$DMC (H$\mathbf{L_B}$, **10**), where Pipp = *para*-isopropylphenyl and DMC = 3,6-dimethylcarbazole, are reported. Dialkyl lutetium complexes of **3** and **10** were prepared in the presence of DMAP and THF by reaction of the proteo ligands with the new trialkyl reagent, Lu(CH_2SiMe_3)$_3$(DMAP)$_2$ (**4**) as well as Lu(CH_2SiMe_3)$_3$(THF)$_2$. For both ligands **3** and **10**, the resulting lutetium complexes were prone to intramolecular cyclometalative alkane elimination reactions whereby the location of cyclometalation was influenced by the identity of the ancillary ligand coordinated to the metal. For ligand **3**, cyclometalation of two PMe_2 groups generated the complex ($\mathbf{L_A}$-κ^3N,κ^2C)Lu(DMAP)$_2$ (**5**), whereas ligand **10** resulted in the single ortho-metalation of a *para*-isopropylphenyl ring to afford ($\mathbf{L_B}$-$\kappa^3N,\kappa C$)Lu(CH_2SiMe_3) (**12**). When complexed with scandium, ligand **10** behaved differently; double cyclometalation of two phospholane moieties resulted in the species ($\mathbf{L_B}$-κ^3N,κ^2C)Sc (**15**). The nature of the cyclometalation reactivity of ligands **3** and **10** is supported by X-ray crystallography and kinetic analysis, respectively.

Key words: ligand design, rare earth, scandium, lutetium, phosphinimine, cyclometalation.

Résumé : Les présents travaux rendent compte de la synthèse et de la réactivité de deux nouveaux ligands de type bis(phosphinimine)carbazole, (PippN=PMe_2)$_2$DMC (H$\mathbf{L_A}$, **3**) et le (PippN=$P(C_4H_8)$)$_2$DMC (H$\mathbf{L_B}$, **10**), où Pipp = *para*-isopropylphényle et DMC = 3,6-diméthylcarbazole. Les complexes de dialkylluthénium dérivés des ligands **3** et **10** ont été préparés en présence DMAP ou de THF par réaction des protéoligands avec le nouveau réactif trialkylé Lu(CH_2SiMe_3)$_3$(DMAP)$_2$ (**4**) ou avec le réactif Lu(CH_2SiMe_3)$_3$(THF)$_2$. Dans le cas des deux ligands (**3** et **10**), les complexes de lutécium obtenus étaient sensibles aux réactions intramoléculaires d'élimination d'alcane par cyclométallation, par lesquelles la position de la cyclométallation était influencée par la nature du ligand auxiliaire coordonné au métal. Dans le cas du ligand **3**, la cyclométallation de deux groupements PMe_2 a produit le complexe ($\mathbf{L_A}$-κ^3N,κ^2C)Lu(DMAP)$_2$ (**5**) tandis que le ligand **10** a subi l'*ortho*-métallation d'un seul cycle *para*-isopropylphényle, produisant le complexe ($\mathbf{L_B}$-$\kappa^3N,\kappa C$)Lu(CH_2SiMe_3) (**12**). Le ligand **10**, lorsque complexé avec le scandium, s'est comporté différemment : une double cyclométallation des deux groupements phospholane a produit l'espèce ($\mathbf{L_B}$-κ^3N,κ^2C)Sc (**15**). La nature de la réactivité des ligands **3** et **10** face à la cyclométallation a été élucidée par radiocristallographie et analyse cinétique, respectivement.

Mots-clés : conception de ligand, terres rares, scandium, lutécium, phosphinimine, cyclométallation.

Introduction

A fine balance is required when tuning the steric properties of an ancillary ligand for use in rare earth metal chemistry. Sufficiently sterically demanding groups must be retained on the ligand for the purpose of shielding the metal centre; however, too much bulk can result in extreme steric crowding and undesired ligand reactivity, such as cyclometalative C–H bond activation.[1] Our group previously developed a family of carbazole-based bis(phosphinimine) ancillaries that offer varying steric and electronic properties. We reported the synthesis of a range of bis(phosphinimine)carbazole pincers whereby the phosphinimine functionality was comprised of two phenyl rings attached to phosphorus, and an aryl group (phenyl, *para*-isopropylphenyl, mesityl, or pyrimidine) bound to nitrogen (**i**, Chart 1) or a dioxaphospholane ring, and a *para*-isopropylphenyl moiety at the nitrogen atom (**ii**, Chart 1).[2] The rare earth complexes of ligand **i** (Ph, Pipp and Mes) were prone to decomposition via intramolecular cyclometalative C–H bond activation of either P-phenyl or N-aryl rings of the ligand.[2a,2d,3] Despite systematic modification of the N-aryl rings of the ligand framework, the pincer retained its tendency toward cyclometalation, with reactivity largely occurring at the PR_2 sites. Accordingly, we have focused our attention at modulation of the ligand framework at phosphorus.

It was expected that a reduction of steric bulk around the exterior edge of the ligand would dampen cyclometalation pathways. For this purpose, a variety of alternatives to the diphenylphosphine subunit (**iii**, Chart 2) were considered. For example, incorporation of dimethylphosphine groups (**iv**, Chart 2) were anticipated to result in significantly reduced peripheral steric properties. This structural change was also expected to integrate other beneficial qualities into the ligand framework, such as improved ligand solubility in aliphatic solvents and diagnostic $^2J_{HP}$ NMR coupling.

In addition to a reduction in steric bulk, it was speculated that linking the R groups on phosphorus together might also reduce the propensity for cyclometalation reactions of the phosphinimine functionality. The intention of this approach was to

Received 29 July 2015. Accepted 7 October 2015.

K.R.D. Johnson, B.L. Kamenz, and P.G. Hayes. Department of Chemistry and Biochemistry, University of Lethbridge, 4401 University Drive, Lethbridge, AB T1K 3M4, Canada.

Corresponding author: Paul G. Hayes (e-mail: p.hayes@uleth.ca).

This article is part of a Special Issue dedicated to celebrating the 50th Anniversary of the Department of Chemistry at the University of Calgary and to highlighting the chemical research being performed by faculty and alumni.

Chart 1. Bis(phosphinimine)carbazole proteo ligands.

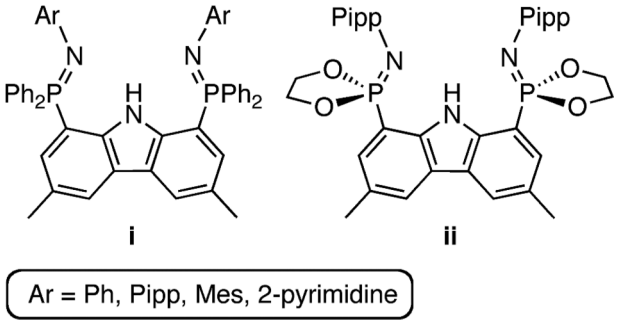

Chart 2. Various $-PR_2$ moieties.

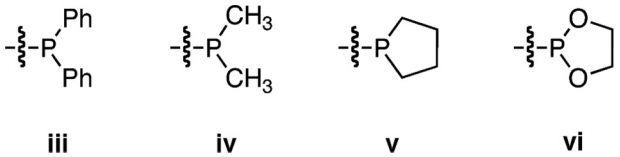

generate a cyclic phosphorus-containing ring with a constrained geometry so that metalative C–H bond activation would be restricted by raising the energy barrier for a highly ordered σ-bond metathesis transition state. We previously explored the use of dioxaphospholane rings for this purpose (**ii**, Chart 1; **vi**, Chart 2); however, it was found that a dialkyl lutetium complex of ligand **ii** was prone to ring opening insertion of the dioxaphospholane rings into lutetium alkyl bonds.[2c] Accordingly, the non-oxygen containing congener, phospholane (**v**, Chart 2), was considered. Notably, the phospholane ring possesses a restricted geometry that was expected to be less prone to pivot to within close proximity of a chelated metal, as required for cyclometalative C–H bond activation at the site adjacent to phosphorus. Thus, an investigation regarding the effect of incorporating dimethylphosphine and phospholane into our bis(phosphinimine)carbazole ligand framework and, subsequently, the potential for these new ligands to support highly reactive rare earth dialkyl species, was undertaken.

Results and discussion

Dimethylphosphine ligand synthesis

The phosphonite ester P–O reactivity of the dioxaphospholane rings in 1,8-di(1,3,2-dioxaphospholan-2-yl)-3,6-dimethyl-9*H*-carbazole (**1**)[2c] with organometallic reagents was exploited to derivatize phosphorus with methyl groups. Reaction of **1** with 5 equiv. of methyllithium in a toluene/THF mixture at 100 °C, followed by aqueous workup, resulted in clean formation of 1,8-bis(dimethylphosphino)-3,6-dimethyl-9*H*-carbazole (**2**) in 81.4% yield. Subsequent reaction of **2** with *para*-isopropylphenyl (Pipp) azide liberated ligand HL_A (**3**) with concomitant loss of dinitrogen (Scheme 1).

The $^{31}P\{^1H\}$ NMR spectrum (benzene-d_6) of proteo ligand **3** exhibits a single resonance at δ 5.4, and the ^1H NMR spectrum (chloroform-*d*) supports the expected structure. In particular, a diagnostic doublet at δ 1.82, corresponding to the P-methyl groups ($^2J_{HP}$ = 12.7 Hz, 12H), was observed. The methyl groups on carbazole give rise to a singlet at δ 2.55 (6H), and the NH proton resonates as a broad singlet at δ 11.18 (1H). In addition to full characterization of **3** by multinuclear NMR spectroscopy, its solid-state structure was also determined by single-crystal X-ray diffraction. The molecular structure is depicted in Fig. 1 as a thermal ellipsoid plot, and selected metrical parameters are listed in Table 1.

Ligand **3** adopts a comparable solid-state structure to the other related structurally characterized proteo ligands described previously.[2] Specifically, one phosphinimine group (N3–P2) is held periplanar to the dimethylcarbazole backbone (N3–P2–C8–C7 torsion angle of 170.8(2)°), whereas the other (N1–P1) is rotated away from the aromatic plane (N1–P1–C1–C2 torsion angle of 147.9(2)°). Relatively long hydrogen bond contacts exist between the carbazole N–H and the nitrogen atoms of both phosphinimine subunits (d(N2···N1) = 2.972(2) Å and d(N2···N3) = 3.010(2) Å). The phosphinimine double bond lengths in **3** are similar to each other, with distances of 1.580(1) Å and 1.579(1) Å for N1–P1 and N3–P2, respectively.

Dimethylphosphine ligand reactivity

To probe the ability of ligand **3** to support dialkyl lutetium complexes, it was reacted with $Lu(CH_2SiMe_3)_3(THF)_2$ in benzene-d_6 at ambient temperature and the reaction was monitored by ^1H and $^{31}P\{^1H\}$ NMR spectroscopy. Unfortunately, the result of this experiment was a mixture of ill-defined products. It is probable that the reaction initially proceeded as expected to afford the alkane elimination product (L_A-κ^3*N*)$Lu(CH_2SiMe_3)_2$; however, this species was likely extremely thermally unstable and rapidly decomposed via unknown routes. It is possible that the complex decomposed by a combination of intra- and intermolecular ligand cyclometalation of N-aryl rings and (or) P-methyl groups, but this has not been established because of the complexity of the resultant mixture of products.

It was reasoned that incorporation of additional σ-donor ligands into the complex would assist in stabilizing an organometallic complex of L_A. Since the two equivalents of THF present in the reaction mixture of proteo ligand **3** and $Lu(CH_2SiMe_3)_3(THF)_2$ did not impart significant stability on the putative dialkyl product, a new lutetium starting material bearing stronger σ-donors was sought.

With two THF donors, $Lu(CH_2SiMe_3)_3(THF)_2$ is thermally sensitive and decomposes at a moderate rate at ambient temperature. However, replacement of the THF ligands with more strongly electron-donating groups has yielded complexes with improved thermal sensitivity, such as (*t*-Bu_2bpy)$Lu(CH_2SiMe_3)_3$,[4] (*i*-Pr-trisox)$Lu(CH_2SiMe_3)_3$,[5] and (12-crown-4)$Lu(CH_2SiMe_3)_3$,[6] where *t*-Bu_2bpy = 4,4′-di-*tert*-butyl-2,2′-bipyridyl, *i*-Pr-trisox = 1,1,1-tris[(*S*)-4-isopropyloxazolinyl]ethane, and 12-crown-4 = 1,4,7,10-tetraoxacyclododecane. Similarly, 4-dimethylaminopyridine (DMAP) has proved to be an effective σ-donor ligand in rare earth metal chemistry and was in fact recently celebrated for its role as a Lewis base in stabilizing the first unambiguous example of a terminal scandium imido complex.[7] Accordingly, we aimed to replace the THF moieties in $Lu(CH_2SiMe_3)_3(THF)_2$ with DMAP ligands.

The new complex $Lu(CH_2SiMe_3)_3(DMAP)_2$ (**4**) was readily synthesized by reaction of $Lu(CH_2SiMe_3)_3(THF)_2$ with 2 equiv. of DMAP in toluene solution; the THF byproduct was easily removed under reduced pressure (Scheme 2). In benzene-d_6, the ^1H NMR spectrum of **4** exhibits methylene and methyl signals at δ −0.24 and δ 0.42, integrating to 6H and 27H, respectively. The spectrum also contains a singlet at δ 2.05 attributed to the dimethylamino group of DMAP and two doublets at δ 6.00 and δ 8.74, each integrating to 4H, corresponding to the aromatic DMAP protons.

The solid-state structure of **4**, elucidated by single-crystal X-ray diffraction (Fig. 2; Table 2) revealed a monomeric, five-coordinate lutetium centre with geometry that is best described as distorted trigonal bipyramidal. As anticipated, the three sterically demanding alkyl groups lie in the equatorial plane (C26–Lu1–C22 = 114.6(1)°, C22–Lu1–C18 = 133.7(1)°, and C18–Lu1–C26 = 111.7(1)°), and the two DMAP ligands occupy the apical sites (N1–Lu1–N3 = 177.3(1)°). The Lu–C bond lengths (2.373(3), 2.384(3), and 2.354(3) Å) and Lu–C–Si bond angles (126.5(2)°, 123.0(2)°, and 129.8(2)°) are

Can. J. Chem. Downloaded from www.nrcresearchpress.com by University of Lethbridge on 04/11/16
For personal use only.

Scheme 1. Synthesis of dimethylphosphine-substituted ligand (PippN=PMe_2)$_2$DMC (**3**).

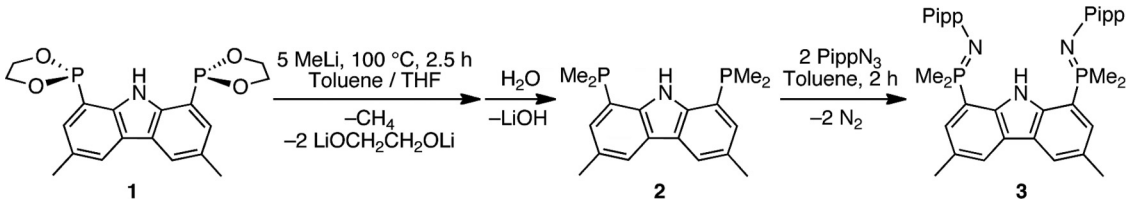

Fig. 1. Thermal ellipsoid plot (50% probability) of (PippN=PMe_2)$_2$DMC (**3**) with hydrogen atoms (except H2N) omitted for clarity.

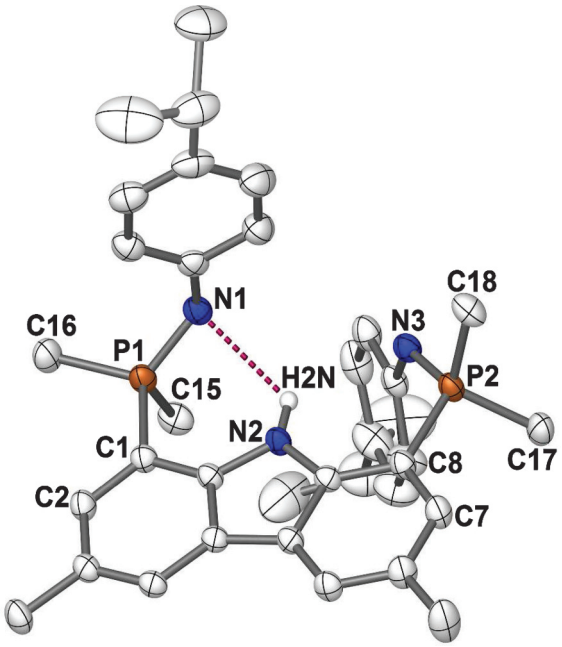

Table 1. Selected bond distances, angles, and torsion angles for compound **3** ((PippN=PMe_2)$_2$DMC).

Bond distance (Å)	
P1–C15	1.788(2)
P2–C17	1.805(2)
C1–P1	1.808(2)
N1–P1	1.580(1)
N2···N1	2.972(2)
P1–C1	1.806(2)
P2–C18	1.793(2)
C8–P2	1.809(2)
N3–P2	1.579(1)
N2···N3	3.010(2)
Bond angle (°)	
C15–P1–C16	105.1(1)
C1–P1–C15	107.0(1)
C8–P2–C17	105.1(1)
C1–P1–N1	111.83(8)
C17–P2–C18	105.8(1)
C1–P1–C16	106.3(1)
C8–P2–C18	106.4(1)
C8–P2–N3	115.36(7)
Torsion angle (°)	
C2–C1–P1–C15	–95.6(2)
C2–C1–P1–C16	16.2(2)
C7–C8–P2–C17	40.5(2)
C7–C8–P2–C18	–71.4(2)
C2–C1–P1–N1	147.9(2)
C7–C8–P2–N3	170.8(2)

Scheme 2. Synthesis of Lu(CH_2SiMe_3)$_3$(DMAP)$_2$ (**4**).

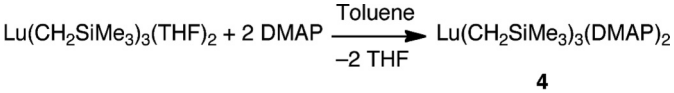

Fig. 2. Thermal ellipsoid plot (50% probability) of Lu(CH_2SiMe_3)$_3$(DMAP)$_2$ (**4**) with hydrogen atoms omitted for clarity.

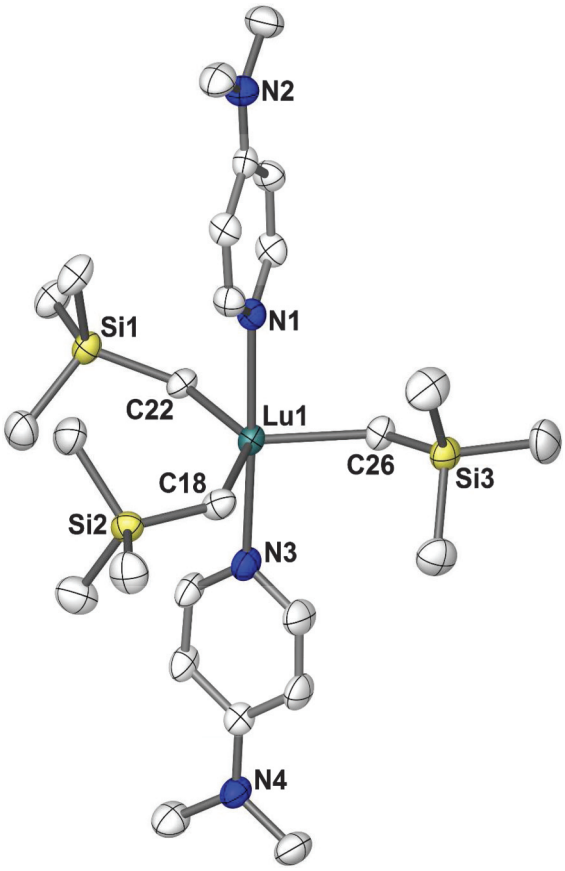

comparable to other lutetium complexes containing three trimethylsilylmethyl ligands.[4,5,6]

Reaction of complex **4** with proteo ligand **3** proceeded cleanly at ambient temperature to afford a single product (**5**) (Scheme 3). From the ^{1}H NMR spectrum of **5**, it was evident that the product was a doubly cyclometalated complex, ($\mathbf{L_A}$-κ^3N,κ^2C)Lu(DMAP)$_2$, whereby the ligand was coordinated via three nitrogen atoms and two metalated P-methyl groups. Particularly diagnostic features in the ^{1}H NMR spectrum (benzene-d_6) of **5** include the P-methyl signal, which appears as a doublet at δ 1.99 ($^2J_{HP}$ = 12.4 Hz) and integrates to 6H, and the cyclometalated P–CH_2 moieties, which resonate as a multiplet at δ 0.58 with an integration of 4H.

It is probable that the reaction of **4** with proteo ligand **3** proceeded with initial loss of 1 equiv. of tetramethylsilane to form a putative dialkyl complex of the ligand, ($\mathbf{L_A}$-κ^3N)Lu(CH_2SiMe_3)$_2$(DMAP)$_n$, (n = 0, 1,

Can. J. Chem. Downloaded from www.nrcresearchpress.com by University of Lethbridge on 04/11/16
For personal use only.

Can. J. Chem. Downloaded from www.nrcresearchpress.com by University of Lethbridge on 04/11/16
For personal use only.

Table 2. Selected bond distances and angles for compound **4** ($Lu(CH_2SiMe_3)_3(DMAP)_2$).

Bond distance (Å)	
C18–Lu1	2.373(3)
C22–Lu1	2.384(3)
C26–Lu1	2.354(3)
N1–Lu1	2.408(3)
N3–Lu1	2.414(3)
Bond angle (°)	
C26–Lu1–C22	114.6(1)
C22–Lu1–C18	133.7(1)
C18–Lu1–C26	111.7(1)
N1–Lu1–N3	177.3(1)
Si1–C22–Lu1	126.5(2)
Si3–C26–Lu1	123.0(2)
Si2–C18–Lu1	129.8(2)

Scheme 3. Synthesis of doubly cyclometalated complex ($(\mathbf{L_A}\text{-}\kappa^3N,\kappa^2C)Lu(DMAP)_2$ (**5**).

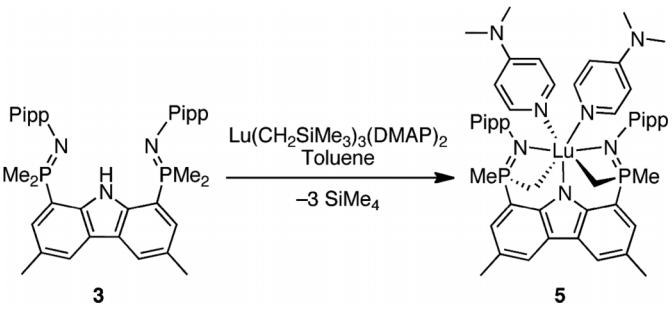

or 2). Subsequent cyclometalation of two P-methyl groups and loss of another 2 equiv. of tetramethylsilane would liberate the final doubly cyclometalated complex **5**. Similar reactivity was previously documented in a scandium dimethyl complex of an anilido phosphinimine ligand, whereby cyclometalation of a dimethylphosphine group occurred with loss of 1 equiv. of methane.[8]

To unambiguously confirm the identity of complex **5**, an X-ray diffraction experiment was performed. Single crystals of the compound were obtained by slow diffusion of pentane into a benzene solution, and it was found to crystallize in the monoclinic space group $P2_1/c$. The molecular structure of **5** is depicted in Fig. 3, and selected metrical parameters are listed in Table 3.

The metal centre in **5** is seven-coordinate and adopts a distorted pentagonal bipyramidal geometry with the equatorial plane defined by N1, C16, N4, N3, and C18 (N1–Lu1–C16 = 62.70(6)°, C16–Lu1–N4 = 72.92(7)°, N4–Lu1–N3 = 75.29(6)°, N3–Lu1–C18 = 63.58(7)°, and C18–Lu1–N1 = 89.53(7)°) and the apical positions occupied by N2 and N6 (N2–Lu1–N6 = 163.42(6)°).

The Lu–C bond lengths in complex **5** are quite long (2.548(2) and 2.529(2) Å) and are comparable to the Lu–C bond distances in a phosphonium bis(ylide) complex, $Cp^*Lu((CH_2)_2PPh_2)_2$ (2.493(2), 2.526(2), 2.465(2), and 2.480(2) Å).[9] Interestingly, the bonding mode of the N–P–C moieties in **5** has some resemblance to that of a phosphonium ylide ligand. Particularly evident are the short P1–C16 and P2–C18 bond lengths of 1.715(2) and 1.724(2) Å, respectively. These can be compared to the longer P1–C15 and P2–C17 bond distances (1.810(2) and 1.814(2) Å, respectively) as well as the P–Me bonds in **3** (1.788(2), 1.806(2), 1.805(2), and 1.793(2) Å). For this reason, it could be speculated that there is some electron delocalization within the N–P–C moieties of **5**. Unfortunately, limited data exists to support this notion beyond the metrical parameters obtained from the solid-state structure of complex **5**. Evidence that argues against this conjecture includes the NMR chemical shifts for the metalated CH_2 subunits. For example, in the ^1H NMR spectrum of **5**, the CH_2 moiety appears as a multiplet with a chemical shift of δ 0.58. This chemical shift is far more representative of an alkyl-type $-CH_2^-$ ligand bonded to lutetium rather than an olefinic $=CH_2$ group.

In an effort to further derivatize the metal centre of **5**, its acid–base reactivity with a variety of anilines was tested; unfortunately, the complex showed no signs of reactivity towards these substrates, even at elevated temperatures (100 °C, 48 h). It can therefore be surmised that the two DMAP ligands coordinated to the metal centre in **5** stabilize the complex to a degree where it appears to be inert toward such reactivity.

Fig. 3. Thermal ellipsoid plot (50% probability) of $(\mathbf{L_A}\text{-}\kappa^3N,\kappa^2C)Lu(DMAP)_2$ (**5**) with hydrogen atoms and two benzene molecules of crystallization omitted for clarity. Positionally disordered atoms are depicted as spheres of arbitrary radius.

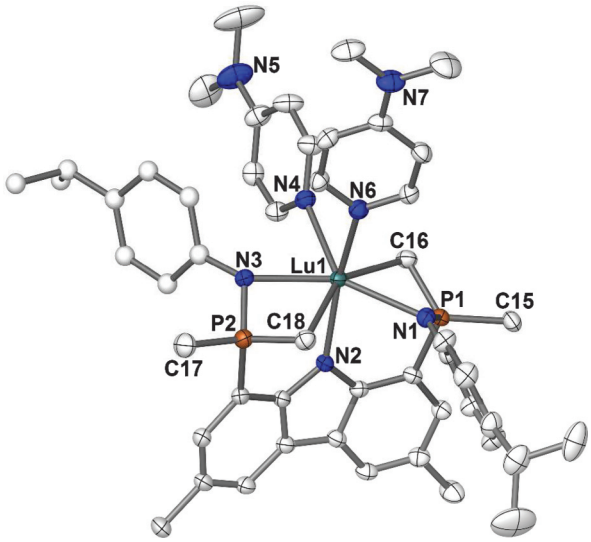

Table 3. Selected bond distances/Å and angles/° for compound **5** ($(\mathbf{L_A}\text{-}\kappa^3N,\kappa^2C)Lu(DMAP)_2$).

Bond distance (Å)	
Lu1–C16	2.548(2)
Lu1–C18	2.529(2)
Lu1–N1	2.393(2)
Lu1–N2	2.325(2)
Lu1–N3	2.391(2)
Lu1–N4	2.445(2)
Lu1–N6	2.413(2)
P1–N1	1.633(2)
P2–N3	1.626(2)
P1–C15	1.810(2)
P1–C16	1.715(2)
P2–C17	1.814(2)
P2–C18	1.724(2)
Bond angle (°)	
N2–Lu1–N6	163.42(6)
N1–Lu1–C16	62.70(6)
C16–Lu1–N4	72.92(7)
N4–Lu1–N3	75.29(6)
N3–Lu1–C18	63.58(7)
C18–Lu1–N1	89.53(7)
C15–P1–C16	119.6(1)
C17–P2–C18	118.1(1)
N1–P1–C15	111.2(1)
N1–P1–C16	100.5(1)
N3–P2–C17	110.5(1)
N3–P2–C18	101.5(1)

Can. J. Chem. Downloaded from www.nrcresearchpress.com by University of Lethbridge on 04/11/16
For personal use only.

Scheme 4. Synthesis of 1-chlorophospholane (**6**).

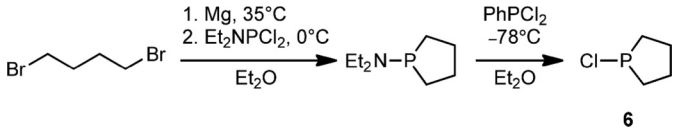

Phospholane ligand

Because of the propensity of ligand $\mathbf{L_A}$ to undergo cyclometalation of its PMe_2 groups to afford complexes of type **5**, we were interested in further modifying the ligand structure to limit such chemistry. Accordingly, we premised that linking the alkyl groups on phosphorus together, thus generating a cyclic ring with a constrained geometry, would aid in restricting metalative C–H activation at this site. Whereas a phospholane-based framework was expected to exhibit similar electronic properties as the PMe_2 congener, it was also anticipated that the significantly different geometry would lead to a metalation-resistant phosphinimine ligand.

The phospholane precursor required for this work, 1-chlorophospholane (**6**), was prepared via a modified literature procedure,[10] wherein the Grignard reagent of 1,4-dibromobutane was reacted with dichloro(diethylamino)phosphine, followed by chlorination with dichlorophenylphosphine (Scheme 4).[10]

Synthesis of the new proteo ligand containing phospholane rings was carried out using a synthetic protocol previously developed by our group from 1,8-dibromo-3,6-dimethyl-9-*t*-BOC-carbazolide (**7**) (Scheme 5).[2a,2c] Installation of phospholane rings onto the carbazole framework was achieved by lithiation of **7** with *t*-BuLi followed by addition of 1-chlorophospholane. Thermal deprotection (155 °C) of the resulting *t*-BOC-protected derivative **8**, liberated bis(phospholane) **9** over 3.5 h. Lastly, in a manner analogous to the preparation of **3**, reaction of **9** with *para*-isopropylphenyl azide generated ligand $\mathbf{HL_B}$ (**10**), with loss of dinitrogen (Scheme 5).

In the $^{31}P\{^1H\}$ NMR spectrum of bis(phospholane) compound **9**, the phospholane groups attached to the 1 and 8 positions of carbazole resonate at δ –35.6 (benzene-d_6), notably downfield from the ^{31}P chemical shift of dimethylphosphine analogue **2** at δ –64.1 (benzene-d_6). In the ^1H NMR spectrum of **9**, the aliphatic region corresponding to the CH_2 groups of the phospholane rings appears as multiple broad overlapping multiplets because of complex H–H and H–P coupling, as well as fluxionality of the phospholane ring on the NMR timescale. This renders the phospholane protons difficult to discern from one another and, therefore, of limited diagnostic value. Proteo ligand **10** exhibits a single resonance in the $^{31}P\{^1H\}$ NMR spectrum at δ 31.3 (benzene-d_6) and displays key signals attributed to the Pipp methine (δ 2.78, sp), Pipp methyl (δ 1.22, d), carbazole methyl (δ 2.36, s), and carbazole NH (δ 12.55, s) in the ^1H NMR spectrum.

Recrystallization of bis(phospholane) **9** from a concentrated pentane solution at ambient temperature yielded large yellow plates suitable for analysis by single-crystal X-ray diffraction. Compound **9** crystallized in the orthorhombic space group *Pbcn* (Fig. 4). The molecule exhibits high symmetry in the solid state, with twofold rotational symmetry about the axis defined by the N1–H1 bond. Owing to this symmetry, the ring system of the phospholane moieties lay on opposite planes of the carbazole scaffold. The phosphorus atoms lay relatively periplanar to the aromatic carbazole backbone, expressed by the N1–C10–C5–P1 torsion angle of 2.9(2)° (Table 4). This geometry is notably different from that in the solid-state structure of the close analogue **1**, which possesses dioxaphospholane rings in place of the phospholane rings in **9**.[2c] In **1**, both dioxaphospholane rings lay on the same plane of the carbazole framework; this arrangement is likely influenced by hydrogen-bonding interactions of the dioxaphospholane oxygen atoms with the carbazole NH. The C5–P1 bond length in **9** is 1.840(2) Å; highly comparable to the analogous C–P bond distances in **1** (1.839(2) and 1.829(2) Å).

Scheme 5. Synthesis of proteo ligand (PippN=P(C_4H_8))$_2$DMC ($\mathbf{HL_B}$, **10**).

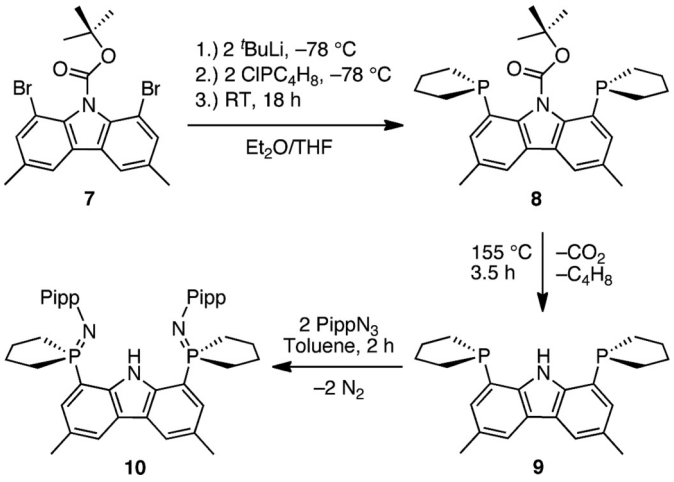

Fig. 4. Thermal ellipsoid plot (50% probability) of bis(phospholane) (**9**) with hydrogen atoms (except H1) omitted for clarity.

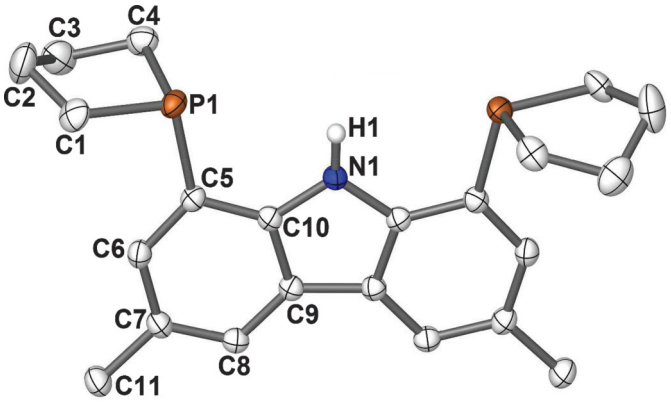

Table 4. Selected bond distances, angles, and torsion angles for bis(phospholane) (**9**).

Bond distance (Å)	
P1–C5	1.840(2)
P1–C4	1.860(2)
P1–C1	1.864(2)
C1–C2	1.542(3)
C2–C3	1.518(3)
C3–C4	1.513(3)
Bond angle (°)	
C4–P1–C1	92.2(1)
C5–P1–C4	101.3(1)
C5–P1–C1	104.2(1)
C2–C1–P1	107.2(1)
C3–C4–P1	106.9(1)
C3–C2–C1	108.5(2)
Torsion angle (°)	
C1–C2–C3–C4	–45.6(2)
N1–C10–C5–P1	2.9(2)

In addition to identification by multinuclear NMR spectroscopy, proteo ligand **10** was structurally characterized by single-crystal X-ray diffraction. Colourless plates of **10** were obtained from a concentrated solution of benzene layered with pentane at ambient temperature. Compound **10** crystallized in the mono-

Can. J. Chem. Downloaded from www.nrcresearchpress.com by University of Lethbridge on 04/11/16
For personal use only.

Fig. 5. Thermal ellipsoid plot (50% probability) of (PippN=P(C_4H_8))$_2$DMC (HL_B, **10**) with hydrogen atoms (except H1) omitted for clarity.

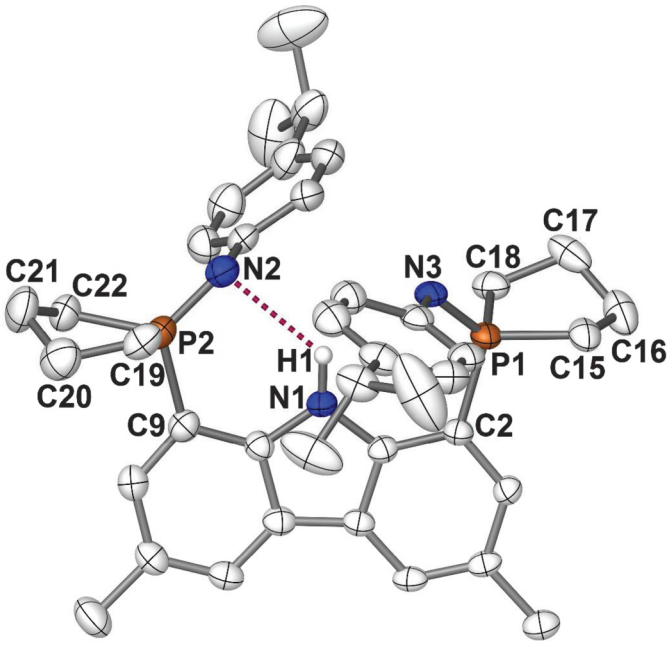

clinic space group *C*2/*c*, with one molecule of benzene and one molecule of pentane, and is illustrated as a thermal ellipsoid plot in Fig. 5. In the solid state, the N-aryl groups of **10** are nearly perpendicular to the planar carbazole backbone; a similar arrangement was observed in the structure of **3**. The phosphinimine P–N bond lengths of **10** are 1.575(3) and 1.572(3) Å for P1–N3 and P2–N2, respectively (Table 5); these distances are highly comparable to those of **3** (1.580(1) and 1.579(1) Å) and consistent with the expected P=N double bond character.[2a–2c,3,11] The bond angles of 95.7(2)° and 95.2(2)° for C18–P1–C15 and C19–P2–C22, respectively, are substantially more acute than the corresponding Me–P–Me bond angles in **3** (105.1(1)° and 105.8(1)° for C15–P1–C16 and C17–P2–C18, respectively). This difference is a testament to the highly constrained geometry of the phospholane rings in **10** and was interpreted as likely to prevent cyclometalation at these sites.

Table 5. Selected bond distances, angles, and torsion angles for (PippN=P(C_4H_8))$_2$DMC (HL_B, **10**).

Bond distance (Å)	
P1–C2	1.807(3)
P2–C9	1.808(3)
P1–N3	1.575(3)
P2–N2	1.572(3)
Bond angle (°)	
C2–P1–N3	112.3(1)
C9–P2–N2	114.4(2)
C18–P1–C15	95.7(2)
C19–P2–C22	95.2(2)
Torsion angle (°)	
C9–P2–N2–C32	72.0(3)
C2–P1–N3–C23	61.4(3)
C1–C2–P1–N3	34.1(3)
C8–C9–P2–N2	23.2(3)

Metal complexation and cyclometalation

In an effort to compare the reactivity of proteo ligands **10** and **3**, Lu(CH_2SiMe_3)$_3$(THF)$_2$ was reacted with **10** to generate the corresponding dialkyl species. This reaction was monitored on NMR-tube scale by multinuclear NMR spectroscopy in benzene-d_6, whereby ligand complexation proceeded cleanly, giving the expected organometallic species (L_B-κ^3*N*)Lu(CH_2SiMe_3)$_2$ (**11**), with liberation of 1 equiv. of $SiMe_4$ and 2 equiv. of THF (Scheme 6).

Compound **11** exhibits a single resonance at δ 54.6 in its ^{31}P{^{1}H} NMR spectrum, consistent with C_{2v} symmetry in solution, wherein the ancillary ligand is bound via a κ^3-coordination mode of the three nitrogen atoms to lutetium. Notably, this signal is about 20 ppm downfield of that observed for proteo ligand **10** (δ 31.3, benzene-d_6). A similar relative change in the ^{31}P NMR resonance of **3** was also observed upon complexation; this is a testament to the sensitivity of the phosphinimine functionality to its chemical environment. In the ^{1}H NMR spectrum of **11**, the methylene and $SiMe_3$ signals for the metal-bound alkyls appear as single resonances at δ –0.57 and δ 0.14, respectively, in deuterated benzene, indicating that both groups are equivalent on the NMR timescale. Although 2 equiv. of THF were present in the reaction mixture, the chemical shifts of the THF resonances do not suggest coordination to the metal centre.

Although the dialkyl lutetium complex **11** was successfully generated in situ and fully characterized in this form by multinuclear NMR spectroscopy, it was found to be thermally unstable and, over time, decomposed with loss of a second equivalent of $SiMe_4$ (vide infra). Because of this, attempts to isolate **11** as an analytically pure solid were unsuccessful and always resulted in mixtures of **11** and its decomposition product. However, complex **11** can be quantitatively prepared and studied at low temperature.

Under ambient conditions, compound **11** slowly converts to a new species of low symmetry, as evident by the appearance of two resonances of equal intensity in its ^{31}P{^{1}H} NMR spectrum (δ 55.9 and 53.1, benzene-d_6). In addition, the loss of 1 equiv. of $SiMe_4$ was observed at δ 0.00 in the ^{1}H NMR spectrum. Combined, the spectral evidence suggests an intramolecular C–H bond activation, resulting in the production of a singly cyclometalated complex. It is postulated that the metalative process occurs between an ortho C–H bond of the N-aryl ring and lutetium metal centre, yielding the ortho-metalated complex **12** depicted in Scheme 6. Metalated (C_{aryl}–Lu) aromatic carbon atoms, such as those in complex **12**, typically exhibit a characteristic ^{13}C NMR resonance at about δ 200 (e.g., $LuPh_3(THF)_2$ (δ 198.7, benzene-d_6),[12] Lu(*p*-tol)$_3$(THF)$_2$ (δ 195.2, benzene-d_6),[12] Lu(C_6H_4-*p*-Et)$_3$(THF)$_2$ (δ 194.2, benzene-d_6),[12] (Cp*)$_2$LuPh (δ 198.5, cyclohexane-d_{12}),[13] Lu(*o*-$C_6H_4CH_2NMe_2$)$_3$ (δ 196.7, benzene-d_6),[14] ($\mathbf{L_C}$-κ^3*N*,κ^{2}C^{Pipp})Lu(THF) (δ 204.7, dd, $^2J_{CP}$ = 40.9 Hz, $^4J_{CP}$ = 1.2 Hz),[2a] and ($\mathbf{L_C}$-κ^3*N*,κ*C*$^{N\text{-}Pipp}$)Lu(NHMes*) (δ 182.8, d, J_{CP} = 21.7 Hz, benzene-d_6),[3] where $\mathbf{L_C}$ = 1,8-(PippN=PPh_2)$_2$DMC, **i**)). With respect to **12**, we were unable to detect a resonance in the ^{13}C NMR spectrum indicative of a typical C_{aryl}–Lu bond; however, multiple factors may have hindered the observation of an already weak quaternary signal. For example, P–C coupling between the metalated carbon atom and both phosphorus nuclei in the molecule would give rise to a doublet of doublet, thus diminishing its intensity and potentially rendering it indiscernible from baseline noise. In other related metalated lutetium complexes developed by our group, we have found that the ortho-metalated carbon signal can be notoriously difficult to observe, even when sophisticated two-dimensional NMR experiments were employed. In fact, we have only been able to locate such resonances previously when thermally stable cyclometalated products could be isolated as well-behaved solids.[2a,3] We have ruled out the possibility of cyclometalation occurring at the phospholane rings in a manner similar to that which occurred in complex **5**. Specifically, the number, integration, and multiplicity exhibited for both the aromatic *para*-isopropylphenyl (7H) and phospholane methylene (16H) protons match that expected for a C_1-symmetric complex that is singly metalated at the ortho position of a Pipp group.

Scheme 6. Synthesis of (L_B-κ³*N*)Lu(CH_2SiMe_3)$_2$ (**11**) and intramolecular C–H bond activation to form (L_B-κ³*N*,κ*C*)Lu(CH_2SiMe_3) (**12**).

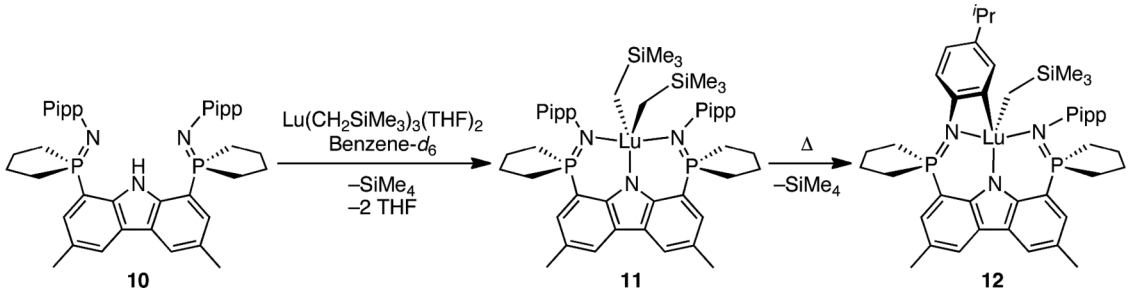

Following decomposition of **11** to the singly metalated compound **12**, further degradation to a series of unknown species (possibly double cyclometalation products) was observed by spectroscopic analysis. The instability of the N-aryl metalated compound **12** made its full characterization extremely difficult, even at low temperatures, and isolation of a well-behaved solid was not possible. The complicated nature of this mixture of decomposition products has precluded their identification.

Kinetic analysis of ligand metalation

The decomposition of complex **11** to **12** was quantitatively monitored using $^{31}P\{^1H\}$ NMR spectroscopy in toluene-d_8, revealing the process to be first order in dialkyl **11** across the broad temperature range of 271.3–315.7 K. The reaction progress, studied by $^{31}P\{^1H\}$ NMR spectroscopy at 295.3 K, is illustrated in Fig. 6, whereby disappearance of the peak at δ 54.6 (corresponding to compound **11**) along with simultaneous emergence of two resonances of equal intensity at δ 55.9 and 53.1 (attributed to the asymmetric product **12**) was observed over 10 800 s.

The observed rate constants for the cyclometalation of complex **11** were obtained from first-order plots of the reaction with observed $t_{1/2}$ values ranging from 7.7 h to 3.7 min (Table 6). To express the temperature dependence of the observed rate constants, an Eyring plot was constructed (Fig. 7), which allowed for extraction of the activation parameters $\Delta H^‡ = 74.50 \pm 0.58$ kJ mol^{-1} and $\Delta S^‡ = -58.13 \pm 0.97$ J K^{-1} mol^{-1}. Notably, the enthalpic and entropic activation values for the reaction of **11** to **12** agree well with those determined for similar ortho-metalation reactions,[2a,3] implying an analogous σ-bond metathesis transition state.

Scandium complexation and cyclometalation

Preliminary results demonstrated that scandium complexes of ligand **10** behave markedly different from the lutetium congeners described in the previous section. A dialkyl scandium complex (L_B-κ³*N*)Sc(CH_2SiMe_3)$_2$ (**13**) was prepared in situ by reaction of Sc(CH_2SiMe_3)$_3$(THF)$_2$ with 1 equiv. of proteo ligand **10** in benzene-d_6 at ambient temperature (Scheme 7). As found in the lutetium analogue, scandium appears to be chelated in a symmetric κ³ fashion, which is evident by only one resonance at δ 55.0 in the $^{31}P\{^1H\}$ NMR spectrum (benzene-d_6). In the ^1H NMR spectrum, the scandium methylene moieties appear slightly upfield of tetramethylsilane at δ –0.19.

As shown in the stacked plot of $^{31}P\{^1H\}$ NMR spectra presented in Fig. 8, complex **13** slowly degrades under ambient conditions. Over time, the resonance at δ 55.0 decreases in intensity as the simultaneous appearance of two new peaks at δ 53.0 and δ 56.1 are observed in a 1:1 ratio, suggesting the formation of a new compound with low symmetry. Finally, disappearance of the resonances at δ 53.0 and δ 56.1 occurs with the concomitant emergence of a single resonance at δ 56.2, which is attributed to the formation of either a C_{2v} or C_s symmetric compound.

Although the $^{31}P\{^1H\}$ NMR spectral data do not provide significant structural information about the final decomposition product, analysis of ^{13}C NMR data has allowed for the unambiguous determination of a doubly metalated Sc complex (**15**), whereby

Fig. 6. Stacked plot of $^{31}P\{^1H\}$ NMR spectra following the decomposition of (L_B-κ³*N*)Lu(CH_2SiMe_3)$_2$ (**11**) to (L_B-κ³*N*,κ*C*)Lu(CH_2SiMe_3) (**12**) at 296.2 K from t = 300 s to t = 10 800 s.

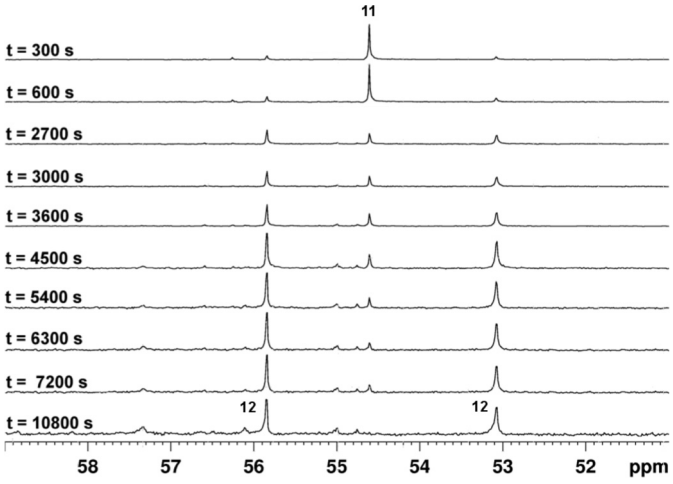

Table 6. Observed rate constants and half-lives for the intramolecular cyclometalation of (L_B-κ³*N*)Lu(CH_2SiMe_3)$_2$ (**11**) to (L_B-κ³*N*,κ*C*)Lu(CH_2SiMe_3) (**12**) at temperatures ranging from 271.3 to 315.7 K.

T (K)	k (s^{-1})	$t_{1/2}$ (h)
271.3	2.50×10^{-5}	7.70
282.4	8.80×10^{-5}	2.19
296.2	3.74×10^{-4}	0.51
304.6	9.63×10^{-4}	0.20
315.7	3.10×10^{-3}	0.062

Fig. 7. Eyring plot of the cyclometalation of complex **11** ((L_B-κ³*N*)Lu(CH_2SiMe_3)$_2$).

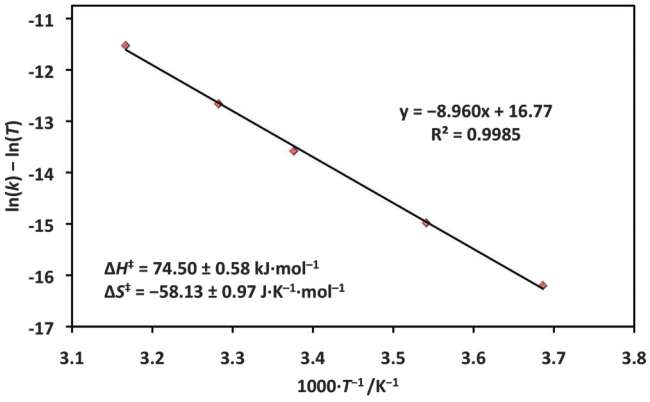

Can. J. Chem. Downloaded from www.nrcresearchpress.com by University of Lethbridge on 04/11/16
For personal use only.

Scheme 7. Synthesis of (L_B-κ^3*N*)Sc(CH_2SiMe_3)$_2$ (**13**) and decomposition to complex **15** ((L_B-κ^3*N*,κ^2*C*)Sc) through two sequential intramolecular cyclometalation processes.

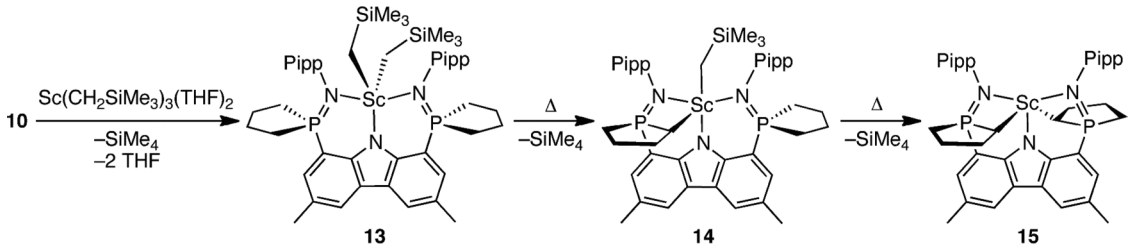

Fig. 8. Stacked plot of the decomposition of (L_B-κ^3*N*)Sc(CH_2SiMe_3)$_2$ (**13**) followed by $^{31}P\{^1H\}$ NMR spectroscopy at 294.2 K.

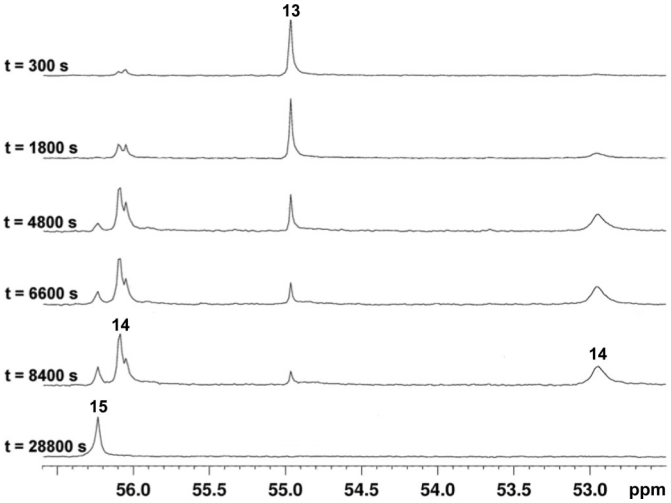

cyclometalation occurs through the phospholane rings. In particular, DEPT–NMR characterization techniques were instrumental, because the CH_2 region corresponding to the phospholane groups was of significant interest. For example, in the DEPT-135 NMR spectrum of **15**, a total of three resonances corresponding to CH_2 groups of the phospholane rings were observed. If no metalation had occurred, only two unique CH_2 phospholane resonances would be present, as found for the proteo ligand **10**. If metalation of only one phospholane group occurred, a spectrum with seven unique CH_2 resonances in the aliphatic region would be expected. The presence of three doublets, however, corresponds to three unique CH_2 chemical environments, which can only occur by cyclometalation of one CH_2 group from each phospholane. The coupling constants of the remaining methylene resonances correspond to expected values for one- and two-bond J_{CP} coupling ($^1J_{CP}$ = 43.85 Hz; $^2J_{CP}$ = 3.78 and 17.39 Hz), similar to the J_{CP} coupling constants observed in **10** ($^1J_{CP}$ = 64.26 Hz; $^2J_{CP}$ = 11.34 Hz).

Detection of the metalated Sc–CH was difficult by traditional ^{13}C NMR spectroscopy because ^{45}Sc is a quadrupolar nucleus (I = 7/2, 100% abundant) that often causes substantial line broadening in the resonances of adjacent nuclei. In addition, the presence of $^1J_{CP}$ coupling decreases the overall intensity of such peaks. Finally, a CH_2 resonance from the phospholane coincidentally had an identical ^{13}C chemical shift as the metalated Sc–CH group, thus partially obscuring the broad CH resonance. For these reasons, the Sc–CH was not readily observed in either the $^{13}C\{^1H\}$ or DEPT-135 NMR spectrum of **15**. Through the use of a DEPT-90 NMR experiment, however, removal of the overlapping CH_2 signal allowed for clear visualization of the metalated carbon, which resonates at δ 32.2.

Additional evidence that complex **15** is cyclometalated through its phospholane rings and not the *para*-isopropylphenyl groups (as in **12**) was observed in the ^1H NMR spectrum, whereby clear resonances for unperturbed, non-cyclometalated *para*-isopropylphenyl rings appears as two doublets, each integrating to 4H.

The formation of complex **15** presumably occurred by two sequential cyclometalative C–H bond activations of the phospholane rings (Scheme 7). Following formation of the dialkyl compound **13**, cyclometalation most likely proceeds via one phospholane ring to give the asymmetric intermediate **14**, which resonates as two signals at δ 53.0 and δ 56.1 in the $^{31}P\{^1H\}$ NMR spectrum. The ^1H NMR data supports the formation of a low-symmetry compound, as well as the loss of an additional equivalent of $SiMe_4$. Compared to the cyclometalation of **11**, the decomposition of **13** is slower, with complete loss of **13** observed only after 2.5 h at 21.0 °C, and 100% conversion to **15** requiring more than 6 h.

Unfortunately, compound **15** is not thermally stable for prolonged periods in solution at ambient temperature, and further decomposition to a mixture of unidentified substances was observed after a period of 5 h. Although the compound exhibits greater stability at –35 °C, attempts to isolate the double cyclometalated compound yielded a mixture of intractable products.

Conclusion

In an effort to modify a bis(phosphinimine)carbazole ligand, the steric bulk around the peripheral edge of the ligand was reduced by adjusting the R groups at phosphorus. Incorporation of dimethylphosphine moieties afforded ancillary ligand **3**. An alkane elimination reaction of **3** with the new organolutetium reagent Lu(CH_2SiMe_3)$_3$(DMAP)$_2$ (**4**) resulted in the isolation of lutetium complex **5**, which features cyclometalated P-methyl groups. Installation of cyclic phospholane rings at the PR_2 site afforded a unique geometrically constrained ligand **10**. A dialkyl lutetium complex of **10** was prepared; however, it was susceptible to degradation via ortho-metalation of an N-aryl ring of the ancillary. Conversely, a dialkyl scandium complex of **10** was susceptible to double cyclometalation of two phospholane rings at the α-position to phosphorus. From these results, it is evident that even with reduction of steric bulk around the peripheral edge of the bis(phosphinimine)carbazole pincer ligand, and geometric constraints in place, dialkyl rare earth complexes of this framework remain highly susceptible to cyclometalative decomposition. Future generations of this ligand core will clearly require careful design to eliminate accessibility of C–H bonds.

Experimental

General procedures

All reactions were carried out under an argon atmosphere with the rigorous exclusion of oxygen and water using standard glovebox (MBraun) or high vacuum line techniques. The solvents diethyl ether, THF, pentane, heptane, benzene, and toluene were dried and purified using a solvent purification system (MBraun) and distilled under vacuum prior to use from sodium benzophenone ketyl (diethyl ether and THF) or titanocene indicator (pentane, heptane, benzene, and toluene). Deuterated solvents were dried

Can. J. Chem. Downloaded from www.nrcresearchpress.com by University of Lethbridge on 04/11/16
For personal use only.

Can. J. Chem. Downloaded from www.nrcresearchpress.com by University of Lethbridge on 04/11/16
For personal use only.

over sodium benzophenone ketyl (benzene-d_6 and toluene-d_8) or CaH_2 (chloroform-*d*), degassed via three freeze–pump–thaw cycles, distilled under vacuum, and stored over 4 Å molecular sieves under an argon atmosphere. Samples for NMR spectroscopy were recorded on a 300 MHz Bruker Avance II (ultrashield) spectrometer (^{1}H 300.13 MHz, ^{13}C{^{1}H} 75.47 MHz, and ^{31}P{^{1}H} 121.49 MHz) and referenced relative to either $SiMe_4$ through the residual solvent resonance(s) for ^{1}H and ^{13}C{^{1}H} or to external 85% H_3PO_4 for ^{31}P{^{1}H}. All NMR spectra were recorded at ambient temperature (25 °C) unless specified otherwise. Elemental analyses were performed using an Elementar Americas Vario MicroCube instrument. Despite repeated attempts, CHN analysis of the lutetium complex **4** consistently gave values that were low in carbon. Such problems are well known for rare earth complexes and are generally accepted to be the result of the formation of inert carbides.[15] The reagents $Lu(CH_2SiMe_3)_3(THF)_2$,[16] $Sc(CH_2SiMe_3)_3(THF)_2$,[16c,17] **1**,[2c] **7**,[2a] and *para*-isopropylphenyl azide[2a] were prepared according to literature procedures. The reagent MeLi was purchased from Sigma-Aldrich as a 1.6 mol/L solution in Et_2O, and the solvent was removed under vacuum to yield the reagent as a white solid. All other reagents were obtained from commercial sources and used as received.

Synthesis of 1,8-bis(dimethylphosphino)-3,6-dimethyl-9*H*-carbazole (2)

A mixture of toluene and THF (10:1, 20 mL) was added to a 100 mL bomb containing **1** (0.316 g, 0.843 mmol) and MeLi (95.9 mg, 4.36 mmol) at ambient temperature. Initial NH deprotonation occurred immediately at this temperature as evidenced by a rapid colour change from yellow to orange and evolution of methane gas. The vessel was then heated to 100 °C for 2.5 h to promote derivatization at phosphorus. Upon sitting for 10 min and cooling to ambient temperature, a red immiscible ethylene glycoxide layer was evident at the bottom of the vessel. The reaction mixture was transferred by cannula to a two-neck round bottom flask containing degassed H_2O (20 mL) at 0 °C and mixed vigorously. The aqueous layer was removed by cannula, and the clear yellow organic layer was diluted by addition of 50 mL of degassed diethyl ether. The organic layer was dried by addition of $MgSO_4$, and a cannula filtration was performed. All volatile components were removed from the clear yellow solution under reduced pressure to afford a yellow solid. Yield: 0.216 g (81.4%). ^{1}H NMR (benzene-d_6): δ 9.28 (br s, 1H, N*H*), 7.83 (s, 2H, Cz 4,5-C*H*), 7.35 (dd, $^3J_{HP}$ = 5.6 Hz, $^4J_{HH}$ = 1.3 Hz, 2H, Cz 2,7-C*H*), 2.46 (s, 6H, Cz CH_3), 1.15 (d, $^2J_{HP}$ = 2.9 Hz, 12H, P(CH_3)$_2$). ^{13}C{^{1}H} NMR (benzene-d_6): δ 141.8 (d, J_{CP} = 22.6 Hz, Cz *ipso*-*C*), 128.8 (d, J_{CP} = 0.8 Hz, Cz *ipso*-*C*), 127.5 (d, $^2J_{CP}$ = 2.0 Hz, Cz 2,7-CH), 123.1 (dd, J_{CP} = 5.0 Hz, J_{CP} = 2.7 Hz, Cz *ipso*-*C*), 121.7 (d, J_{CP} = 14.3 Hz, Cz *ipso*-*C*), 121.4 (s, Cz 4,5-*C*H), 21.4 (s, Cz *C*H$_3$), 13.4 (d, $^1J_{CP}$ = 11.7 Hz, P(*C*H$_3$)$_2$). ^{31}P{^{1}H} NMR (benzene-d_6): δ –64.1. Anal. Calcd. (%) for $C_{18}H_{23}NP_2$: C, 68.56; H, 7.35; N, 4.44. Found: C, 68.79; H, 7.50; N, 4.48.

Synthesis of HL_A (3)

An aliquot of *para*-isopropylphenyl azide (0.195 g, 1.21 mmol) was added by syringe to a clear yellow solution of **2** (0.184 g, 0.584 mmol) in 10 mL of toluene at ambient temperature. Upon addition, the solution rapidly became turbid with the precipitation of product along with concurrent evolution of nitrogen gas. The yellow suspension was stirred under an argon atmosphere for 3 h, after which the solvent was removed under vacuum and the residue brought into a glovebox. The product was reconstituted in 2 mL of hot toluene and slowly cooled to ambient temperature to recrystallize. Analytically pure pale yellow prisms of **3** were collected by filtration, washed with a minimal amount of cold pentane, and dried thoroughly under reduced pressure. Yield: 0.225 g (66.1%). ^{1}H NMR (benzene-d_6): δ 12.47 (br s, 1H, N*H*), 7.80 (s, 2H, Cz 4,5-C*H*), 7.23 (d, $^3J_{HH}$ = 8.2 Hz, 4H, Pipp C*H*), 7.11 (d, $^3J_{HP}$ = 13.7 Hz, 2H, Cz 2,7-C*H*), 7.06 (d, J_{HH} = 8.2 Hz, 4H, Pipp C*H*), 2.77 (sp, $^3J_{HH}$ = 6.9 Hz, 2H, C*H*(CH$_3$)$_2$), 2.36 (s, 6H, Cz C*H*$_3$), 1.38 (d, $^2J_{HP}$ = 12.6 Hz, 12H, P(C*H*$_3$)$_2$), 1.20 (d, $^3J_{HH}$ = 6.9 Hz, 12H, CH(C*H*$_3$)$_2$). ^{13}C{^{1}H} NMR (chloroform-*d*): δ 149.0 (d, J_{CP} = 4.7 Hz, aromatic *ipso*-*C*), 139.5 (d, J_{CP} = 4.2 Hz, aromatic *ipso*-*C*), 137.3 (s, aromatic *ipso*-*C*), 128.8 (d, J_{CP} = 7.8 Hz, Cz 2,7-*C*H), 128.5 (d, J_{CP} = 10.4 Hz, aromatic *ipso*-*C*), 126.7 (d, J_{CP} = 1.5 Hz, Pipp *C*H), 123.9 (d, J_{CP} = 2.5 Hz, Cz 4,5-*C*H), 123.0 (d, J_{CP} = 7.7 Hz, aromatic *ipso*-*C*), 122.1 (d, J_{CP} = 20.4 Hz, Pipp *C*H), 113.5 (d, J_{CP} = 83.4 Hz, aromatic *ipso*-*C*), 33.0 (s, Pipp *C*H(CH$_3$)$_2$), 24.2 (s, Pipp CH(*C*H$_3$)$_2$), 21.4 (s, Cz *C*H$_3$), 15.6 (d, $^1J_{CP}$ = 72.1 Hz, P(*C*H$_3$)$_2$). ^{31}P{^{1}H} NMR (benzene-d_6): δ 5.4. Anal. Calcd. (%) for $C_{36}H_{45}N_3P_2$: C, 74.33; H, 7.80; N, 7.22. Found: C, 74.47; H, 7.73; N, 7.15.

Synthesis of $Lu(CH_2SiMe_3)_3(DMAP)_2$ (4)

In a glovebox, toluene (3 mL) was added to an intimate mixture of $Lu(CH_2SiMe_3)_3(THF)_2$ (0.270 g, 0.465 mmol) and 4-dimethylaminopyridine (0.115 g, 0.929 mmol) in a small Erlenmeyer flask. The colourless solution was stirred at ambient temperature for 20 min, after which all volatile components were removed under vacuum to yield $Lu(CH_2SiMe_3)_3(DMAP)_2$ as a white solid. Yield: 0.292 g (92.2%). ^{1}H NMR (benzene-d_6): δ 8.74 (d, $^3J_{HH}$ = 6.4 Hz, 4H, DMAP C*H*), 6.00 (d, $^3J_{HH}$ = 6.4 Hz, 4H, DMAP C*H*), 2.05 (s, 12H, DMAP N(C*H*$_3$)$_2$), 0.418 (s, 27H, CH$_2$Si(C*H*$_3$)$_3$), –0.240 (s, 6H, C*H*$_2$Si(CH$_3$)$_3$). ^{13}C{^{1}H} NMR (benzene-d_6): δ 154.6 (DMAP *ipso*-*C*), 149.5 (DMAP *C*H), 106.5 (DMAP *C*H), 42.7 (*C*H$_2$Si(CH$_3$)$_3$), 38.2 (DMAP N(*C*H$_3$)$_2$), 5.1 (CH$_2$Si(*C*H$_3$)$_3$). Anal. Calcd. (%) for $C_{26}H_{53}LuN_4Si_3$: C, 45.86; H, 7.85; N, 8.23. Found: C, 43.51; H, 7.52; N, 8.23.

Synthesis of $(L_A$-$\kappa^3N,\kappa^2C)Lu(DMAP)_2$ (5)

In a glovebox, a 25 mL Erlenmeyer flask was charged with **3** (0.0225 g, 0.0387 mmol) and **4** (0.0265 g, 0.0389 mmol). Benzene (2 mL) was added to the flask and the reaction mixture was stirred at ambient temperature for 1.5 h. The solution was filtered through a bed of Celite, concentrated under reduced pressure to 0.5 mL, and left at ambient temperature to crystallize. The mother liquor was decanted off, leaving small yellow crystals that were washed with a minimal amount of cold pentane and dried under vacuum. Yield: 0.0154 g (39.9%). ^{1}H NMR (benzene-d_6): δ 8.54 (d, $^3J_{HH}$ = 6.4 Hz, 4H, DMAP C*H*), 8.23 (s, 2H, Cz 4,5-C*H*), 7.43 (d, $^3J_{HP}$ = 10.5 Hz, 2H, Cz 2,7-C*H*), 6.88 (d, $^3J_{HH}$ = 8.2 Hz, 4H, Pipp C*H*), 6.74 (d, $^3J_{HH}$ = 8.2 Hz, 4H, Pipp C*H*), 5.84 (d, $^3J_{HH}$ = 6.4 Hz, 4H, DMAP C*H*), 2.66 (s, 6H, Cz CH_3), 2.57 (sp, $^3J_{HH}$ = 6.7 Hz, 2H, C*H*(CH$_3$)$_2$), 2.09 (s, 12H, DMAP N(C*H*$_3$)$_2$), 1.99 (d, $^2J_{HP}$ = 12.4 Hz, 6H, PC*H*$_3$), 1.03 (d, $^3J_{HH}$ = 6.7 Hz, 12H, CH(C*H*$_3$)$_2$), 0.58 (m, 4H, PC*H*$_2$Lu). ^{13}C{^{1}H} NMR (benzene-d_6): δ 154.2 (s, aromatic *ipso*-*C*), 151.9 (d, J_{CP} = 4.1 Hz, aromatic *ipso*-*C*), 151.3 (d, J_{CP} = 6.4 Hz, aromatic *ipso*-*C*), 149.9 (s, DMAP *C*H), 137.8 (s, aromatic *ipso*-*C*), 126.1 (s, Pipp *C*H), 126.0 (d, J_{CP} = 8.9 Hz, Cz 2,7-*C*H), 125.2 (d, J_{CP} = 7.6 Hz, aromatic *ipso*-*C*), 124.4 (d, J_{CP} = 12.9 Hz, Pipp *C*H), 123.7 (d, J_{CP} = 10.4 Hz, aromatic *ipso*-*C*), 123.4 (s, Cz 4,5-*C*H), 121.0 (d, J_{CP} = 82.1 Hz, aromatic *ipso*-*C*), 106.5 (s, DMAP *C*H), 38.2 (s, DMAP N(*C*H$_3$)$_2$), 33.6 (s, Pipp *C*H(CH$_3$)$_2$), 24.6 (s, Pipp CH(*C*H$_3$)$_2$), 22.2 (s, Cz *C*H$_3$), 18.2 (d, $^1J_{CP}$ = 69.9 Hz, PC*H*$_2$Lu), 17.2 (d, $^1J_{CP}$ = 39.5 Hz, PC*H*$_3$). ^{31}P{^{1}H} NMR (benzene-d_6): δ 23.6. Because of the small amount of product obtained, combustion analysis was not performed on this compound.

Synthesis of 1-chlorophospholane (6)

This procedure was modified from the literature.[10] Magnesium turnings (9.09 g, 374 mmol) were added to two-neck 500 mL round-bottom flask equipped with a reflux condenser. Anhydrous diethyl ether (200 mL) was condensed into the flask by vacuum transfer at –78 °C, and the solvent was then brought to reflux at 35 °C. An aliquot of 1,4-dibromobutane (11.2 mL, 93.8 mmol) was added dropwise, and the mixture was continually refluxed at 35 °C for 1.25 h. An additional aliquot of 1,4-dibromobutane (11.2 mL, 93.8 mmol) was then added to the reaction mixture, and it was heated with stirring for a further 1.5 h. The resultant solution was transferred via cannula to a 1 L flask, cooled to –78 °C, and a solution of dichloro(diethylamino)phosphine (24.5 mL,

Can. J. Chem. Downloaded from www.nrcresearchpress.com by University of Lethbridge on 04/11/16
For personal use only.

168 mmol) in diethyl ether (150 mL) was added dropwise to the Grignard solution. The reaction mixture was stirred for 3 h and subsequently transferred to a distillation apparatus by cannula filtration. The remaining magnesium salts were washed with pentane and the pentane washings were combined with the ethereal solution in the distillation apparatus. Both the diethyl ether and pentane were distilled off at 40 °C (oil bath temperature) to yield crude 1-diethylaminophospholane as a yellow oil. The crude oil was transferred to a short-track distillation apparatus and purified by vacuum distillation (~0.01 Torr, 1 Torr = 133.322 Pa) at 96 °C (oil bath temperature). The purified 1-diethylaminophospholane (13.72 g, 86.2 mmol) was added to a 100 mL bomb, where at –78 °C, 11.6 mL (85.5 mmol) of dichlorophenylphosphine was added dropwise. After the addition, the bomb was sealed and cooled at –35 °C for 2 days. The product was then distilled under dynamic vacuum between 60 and 75 °C (oil bath temperature). Yield: 8.57 g (41.6%). ^{1}H NMR (benzene-d_6): δ 1.80 (m, 4H, PCH_2), 1.30 (m, 4H, PCH_2CH_2). ^{31}P{^{1}H} NMR (benzene-d_6): δ 126.4. The NMR data matched that reported in the literature.

Synthesis of *tert*-butyl 3,6-dimethyl-1,8-di(phospholan-1-yl)-9*H*-carbazole-9-carboxylate (8)

A two-neck round bottom flask was charged with **7** (1.01 g, 2.24 mmol), diethyl ether (80 mL), and THF (80 mL) to give a yellow-beige coloured suspension. A pentane solution (1.7 mol/L) of *t*-BuLi (2.63 mL, 4.47 mmol) was added dropwise at –78 °C, and the reaction mixture was stirred at this temperature for 3.5 h, resulting in a colour change to persimmon red. At –78 °C, an aliquot of **6** (0.470 mL, 4.47 mmol) was added, causing the solution to become a light brown colour. The reaction mixture was gradually warmed to ambient temperature with stirring over 18 h, over which time it acquired a cloudy yellow appearance. All volatiles were removed under reduced pressure to leave an orange-yellow solid. The residue was reconstituted in toluene (25 mL), filtered through a fine porosity frit, and the solvent removed in vacuo to afford **8** as a crude residue. This material was used directly in the next step (BOC deprotection) without further purification. Yield: 0.535 g (51.2%) ^{1}H NMR (benzene-d_6): δ 7.30 (s, 2H, Cz 4,5-C*H*), 7.26 (d, $^3J_{HP}$ = 6.7 Hz, 2H, Cz 2, 7-C*H*), 2.50–1.67 (br ov m, 16H, CH_2), 2.23 (s, 6H, Cz CH_3), 1.53 (s, 9H, C(CH_3)$_3$). ^{13}C{^{1}H} (benzene-d_6): 152.9 (s, *C*OO*t*-Bu), 142.9 (d, J_{CP} = 6.0 Hz, aromatic *ipso*-C), 134.8 (d, J_{CP} = 34.9 Hz, aromatic *ipso*-C), 133.7 (d, J_{CP} = 3.1 Hz, aromatic *ipso*-C), 130.5 (d, J_{CP} = 12.4 Hz, aromatic *C*H), 128.9 (s, aromatic *ipso*-C), 118.6 (s, aromatic *C*H), 84.9 (s, *C*(CH$_3$)$_3$), 28.0 (t, J_{CP} = 3.0 Hz, C(*C*H$_3$)$_3$), 27.8 (d, $^2J_{CP}$ = 2.3 Hz, P–CH$_2$*C*H$_2$), 27.7 (d, $^1J_{CP}$ = 10.6 Hz, P–*C*H$_2$CH$_2$), 21.0 (s, Cz *C*H$_3$). ^{31}P{^{1}H} NMR (benzene-d_6): δ –8.9.

Synthesis of 3,6-dimethyl-1,8-di(phospholan-1-yl)-9*H*-carbazole (9)

A solution of **8** (0.535 g, 1.14 mmol) in toluene (30 mL) was loaded into a 100 mL bomb and placed under static vacuum. The amber coloured solution was heated at 155 °C for 3.5 h, then transferred by cannula to a 100 mL round-bottomed flask. The solvent was removed under vacuum to leave the crude product as a yellow oily residue. The material was taken up in pentane (30 mL), filtered, and left at ambient temperature to crystallize. After 24 h, the mother liquor was decanted to afford pale yellow crystals, which were then dried under vacuum. Yield: 0.409 g (96.5%). ^{1}H NMR (benzene-d_6): δ 9.16 (s, 1H, N*H*), 7.81 (s, 2H, Cz 4,5-C*H*), 7.23 (d, $^3J_{HP}$ = 4.0 Hz, 2H, Cz 2,7-C*H*), 2.45 (s, 6H, CH_3), 2.09–1.31 (br ov m, 16H, CH_2). ^{13}C{^{1}H} (benzene-d_6): δ 141.4 (d, J_{CP} = 18.9 Hz, aromatic *ipso*-C), 128.6 (s, aromatic *ipso*-C), 128.0 (s, aromatic *C*H), 123.2 (m, aromatic *ipso*-C), 122.0 (d, J_{CP} = 24.7 Hz, aromatic *ipso*-C), 120.8 (s, aromatic *C*H), 28.3 (d, $^2J_{CP}$ = 3.0 Hz, P–CH$_2$*C*H$_2$), 25.8 (d, $^1J_{CP}$ = 11.3 Hz, P–*C*H$_2$CH$_2$), 21.6 (Ar-*C*H$_3$). δ ^{31}P{^{1}H} NMR (benzene-d_6): δ –35.6. Anal. Calcd. (%) for $C_{21}H_{27}P_2N$: C, 71.92; H, 7.41; N, 3.81. Found: C, 72.14; H, 7.80; N, 4.05.

Synthesis of HL_B (10)

To a solution of **9** (0.203 g, 0.553 mmol) in pentane (30 mL), *para*-isopropylphenyl azide (0.179 g, 1.11 mmol) was added dropwise at ambient temperature. The resulting pale yellow solution was stirred for 18 h, after which, the solvent was removed under reduced pressure. The crude solid was dissolved in a minimal amount of benzene, layered with pentane and left at ambient temperature to recrystallize. Pale yellow crystals of the product were collected by filtration and dried under vacuum. Yield: 0.194 g (58.2%) ^{1}H NMR (benzene-d_6): δ 12.53 (s, 1H, N*H*), 7.79 (s, 2H, Cz 4,5-C*H*), 7.30 (d, $^3J_{HH}$ = 7.9 Hz, 4H, Pipp C*H*), 7.20 (d, $^3J_{HP}$ = 12.5 Hz, 2H, Cz 2,7-C*H*), 7.10 (d, $^3J_{HH}$ = 7.9 Hz, 4H, Pipp C*H*), 2.78 (sp, $^3J_{HH}$ = 6.9 Hz, 2H, C*H*(CH$_3$)$_2$), 2.36 (s, 6H, Cz CH_3), 2.33–1.35 (br ov m, 16H, CH_2), 1.22 (d, $^3J_{HH}$ = 6.9 Hz, 12H, CH(CH_3)$_2$). ^{13}C{^{1}H} NMR (benzene-d_6): δ 150.4 (d, J_{CP} = 4.4 Hz, aromatic *ipso*-C), 140.7 (s, aromatic *ipso*-C), 137.3 (s, aromatic *ipso*-C), 128.4 (d, J_{CP} = 8.8 Hz, aromatic *C*H), 127.9 (s, aromatic *ipso*-C), 126.9 (d, J_{CP} = 1.2 Hz, aromatic *C*H), 123.9 (d, J_{CP} = 2.6 Hz, aromatic *C*H), 123.4 (d, J_{CP} = 7.7 Hz, aromatic *ipso*-C), 123.1 (d, J_{CP} = 19.6 Hz, aromatic *C*H), 113.8 (d, J_{CP} = 85.2 Hz, aromatic *ipso*-C), 33.6 (s, *C*H(CH$_3$)$_2$), 26.7 (d, $^1J_{CP}$ = 63.6 Hz, P–*C*H$_2$CH$_2$), 25.2 (d, $^2J_{CP}$ = 7.5 Hz, P–CH$_2$*C*H$_2$), 24.5 (s, CH(*C*H$_3$)$_2$), 21.3 (s, Cz *C*H$_3$). ^{31}P{^{1}H} NMR (benzene-d_6): δ 31.3. Anal. Calcd. (%) for $C_{40}H_{49}P_2N_3$: C, 75.80; H, 7.79; N, 6.63. Found: C, 75.41; H, 7.66; N, 6.85.

In situ generation of (L_B-κ^3*N*)Lu(CH$_2$SiMe$_3$)$_2$ (11)

An NMR tube was charged with **10** (0.0091 g, 0.014 mmol) and Lu(CH$_2$SiMe$_3$)$_3$(THF)$_2$ (0.0083 g, 0.014 mmol). Benzene-d_6 (0.5 mL) was added to the tube at ambient temperature to afford a pale yellow solution. ^{1}H NMR (benzene-d_6): δ 8.14 (s, 2H, aromatic C*H*), 7.25 (d, $^3J_{HH}$ = 6.5 Hz, 4H, aromatic C*H*), 7.22 (d, $^3J_{HH}$ = 6.5 Hz, 4H, aromatic C*H*), 7.03 (s, 2H, aromatic C*H*), 2.70 (sp, $^3J_{HH}$ = 6.9 Hz, 2H, C*H*(CH$_3$)$_2$), 2.50 (s, 6H, Cz CH_3), 2.12–1.64 (br ov m, 16H, CH_2), 1.16 (d, $^3J_{HH}$ = 6.9 Hz, 12H, CH(CH_3)$_2$), 0.14 (s, 18H, Si(CH_3)$_3$), –0.57 (s, 4H, Lu-CH_2). ^{13}C{^{1}H} NMR (toluene-d_8, 213 K): δ 152.1 (s, aromatic *ipso*-C), 144.2 (d, J_{CP} = 7.1 Hz, aromatic *ipso*-C), 142.7 (s, aromatic *ipso*-C), 137.0 (s, aromatic *ipso*-C), 127.3 (s, Ar-*C*), 126.6 (s, Ar-*C*), 126.5 (s, Ar-*C*), 124.4 (s, Ar-*C*), 124.2 (s, Ar-*C*), 111.6 (d, J_{CP} = 86.1 Hz, aromatic *ipso*-C), 41.0 (s, Lu–*C*H$_2$), 33.9 (s, *C*H(CH$_3$)$_2$), 25.9 (br s, P–CH$_2$CH$_2$), 24.8 (br s, P–CH$_2$CH$_2$), 24.5 (s, CH(*C*H$_3$)$_2$), 21.5 (s, Cz *C*H$_3$), 4.7 (s, Si(*C*H$_3$)$_3$). ^{31}P{^{1}H} NMR (benzene-d_6): δ 54.6. In situ formation and thermal instability of complex **11** rendered analytically pure samples for EA analysis impossible. Therefore, these data were not obtained.

Decomposition of 11 to 12

An NMR tube containing **11** was allowed to sit at ambient temperature over a period of 4 h to generate the asymmetric decomposition product **12**. This decomposition product was also thermally sensitive, resulting in further decomposition to a variety of unknown products at ambient temperature over a time period of 4 h. ^{1}H NMR (benzene-d_6): 8.17 (s, 1H, aromatic C*H*), 8.11 (s, 1H, aromatic C*H*), 7.56 (s, 1H, aromatic C*H*), 7.31 (m, 1H, aromatic C*H*), 7.09 (m, 1H, aromatic C*H*), 7.08 (d, $^2J_{HH}$ = 3.3 Hz, 2H, Pipp C*H*), 7.06 (m, 1H, aromatic C*H*), 6.96 (s, 1H, aromatic C*H*), 6.92 (s, 1H, aromatic C*H*), 6.87 (s, 1H, aromatic C*H*), 2.75–2.66 (ov sp, 2H, CH), 2.56 (s, 3H, Cz CH_3), 2.52 (s, 3H, Cz CH_3), 2.34–1.46 (br ov m, 16H, CH_2), 1.18 (d, $^3J_{HH}$ = 6.9 Hz, 6H, CH_3), 1.14 (d, $^3J_{HH}$ = 6.9 Hz, 6H, CH_3), 0.54 (s, 9H, Si(CH_3)$_3$), 0.47 (s, 2H, Lu–CH_2), ^{31}P{^{1}H} NMR (benzene-d_6): δ 55.9, 53.1. In situ formation and thermal instability of complex **12** rendered acquisition of ^{13}C NMR data and isolation of analytically pure samples for EA analysis impossible. Therefore, these data were not obtained.

In situ generation of (L_B-κ^3*N*)Sc(CH$_2$SiMe$_3$)$_2$ (13)

Compound **11** (0.0097 g, 0.016 mmol) was added to an NMR tube containing Sc(CH$_2$SiMe$_3$)$_3$(THF)$_2$ (0.0072 g, 0.016 mmol) and dissolved in benzene-d_6. The resulting compound slowly decomposed at ambient temperature over a period of 3 h. ^{1}H NMR

Can. J. Chem. Downloaded from www.nrcresearchpress.com by University of Lethbridge on 04/11/16
For personal use only.

Table 7. Summary of crystallography data collection and structure refinement for compounds (PippN=PMe_2)$_2$DMC (**3**), Lu(CH_2SiMe_3)$_3$(DMAP)$_2$ (**4**), ($\mathbf{L_A}$-κ^3*N*,κ^2*C*)Lu(DMAP)$_2$ (**5**), bis(phospholane) (**9**), and (PippN=P(C_4H_8))$_2$DMC (H$\mathbf{L_B}$, **10**).

	3·$C_6H_5CH_3$	**4**	**5**·2 C_6H_6	**9**	**10**[a]·C_6H_6 C_5H_{12}
Formula	$C_{43}H_{53}N_3P_2$	$C_{26}H_{53}LuN_4Si_3$	$C_{62}H_{74}LuN_7P_2$	$C_{22}H_{27}NP_2$	$C_{40}H_{49}N_3P_2$
FW (g mol^{-1})	673.82	680.96	1154.19	367.39	633.76
Crystal system	Triclinic	Triclinic	Monoclinic	Orthorhombic	Monoclinic
Space group	$P\bar{1}$	$P\bar{1}$	$P2_1/c$	*Pbcn*	*C*2/*c*
a (Å)	12.3309(10)	9.7431(11)	11.6505(9)	6.5804(4)	28.899(9)
b (Å)	12.8921(10)	10.3882(12)	21.5593(17)	17.0388(11)	20.046(6)
c (Å)	14.3479(12)	17.970(2)	23.1631(18)	17.1877(11)	15.256(5)
α (°)	72.7090(10)	89.9710(10)	90	90	90
β (°)	65.0130(10)	75.7880(10)	91.0050(10)	90	120.566(3)
γ (°)	72.3270(10)	80.2470(10)	90	90	90
Volume (Å^3)	1931.8(3)	1736.1(3)	5817.1(8)	1927.1(2)	7610(4)
Z	2	2	4	4	8
D_{calcd} (g cm^{-3})	1.158	1.303	1.318	1.266	1.106
μ (mm^{-1})	0.146	2.965	1.796	0.230	0.144
Crystal size (mm^3)	0.57×0.26×0.18	0.28×0.11×0.06	0.54×0.31×0.21	0.25×0.22×0.11	0.21×0.19×0.08
θ range (°)	1.60–27.10	1.99–27.10	1.75–27.10	2.37–27.10	2.56–25.03
N	27 321	19 635	64 976	19 785	44 871
N_{ind}	8478	7597	12 830	2132	6711
Data/restraints/parameters	8478/0/423	7597/0/320	12 830/0/655	2132/0/115	6711/0/413
GoF on F^2	1.036	1.018	1.041	1.097	1.001
$R_1[I > 2\sigma(I)]$[b]	0.0556	0.0306	0.0228	0.0370	0.0766
$wR_2[I > 2\sigma(I)]$[c]	0.1503	0.0588	0.0539	0.0971	0.2090
R_1 (all data)[b]	0.0679	0.0419	0.0272	0.0421	0.1032
wR_2 (all data)[c]	0.1615	0.0624	0.0566	0.1007	0.2292
$\Delta\rho_{max}$ and $\Delta\rho_{min}$ (e Å^{-3})	0.952 and –0.633	0.728 and –1.149	1.516 and –0.984	0.567 and –0.165	0.786 and –0.665

[a]Compound **10** crystallized with two highly disordered solvent molecules (benzene and pentane). The electron density associated with the disordered solvent regions was removed from the reflection file using the SQUEEZE subroutine of PLATON.

[b]$R_1 = \Sigma||F_o| - |F_c||/\Sigma|F_o|$.

[c]$wR_2 = \{\Sigma[w(F_o^2 - F_c^2)^2]/\Sigma[w(F_o^2)^2]\}^{1/2}$.

(benzene-d_6): δ 8.14 (s, 2H, Cz C*H*), 7.04 (m, 4H, Pipp C*H*), 7.02 (m, 4H, Pipp C*H*), 6.98 (s, 2H, Cz C*H*), 2.91 (sp, $^3J_{HH}$ = 6.9 Hz, 2H, C*H*(CH$_3$)$_2$), 2.51 (s, 6H, Cz CH$_3$), 2.15–1.51 (br ov m, 16H, C*H*$_2$), 1.19 (d, $^3J_{HH}$ = 6.9 Hz, 12H, CH(C*H*$_3$)$_2$), 0.02 (s, 18H, Si(C*H*$_3$)$_3$), –0.19 (s, 4H, ScC*H*$_2$). ^{31}P{^{1}H} NMR (benzene-d_6): δ 55.0. In situ formation and thermal instability of complex **13** rendered acquisition of ^{13}C NMR data and isolation of analytically pure samples for EA analysis impossible. Therefore, these data were not obtained.

Decomposition of 13 to 15

An NMR tube containing **13** was left at ambient temperature over a period of 24 h to afford the symmetric, doubly metalated species **15** with the concomitant loss of 2 equiv. of tetramethylsilane. ^{1}H NMR (benzene-d_6): δ 7.85 (s, 2H, Cz 4,5-C*H*), 7.48 (d, $^3J_{HP}$ = 11.1 Hz, 2H, Cz 2,7-C*H*), 7.12 (d, $^3J_{HH}$ = 8.4 Hz, 4H, Pipp C*H*), 6.99 (d, $^3J_{HH}$ = 8.4 Hz, 4H, Pipp C*H*), 2.74 (sp, $^3J_{HH}$ = 6.7 Hz, 2H, C*H*), 2.51 (s, 6H, Cz C*H*$_3$), 2.14–1.23 (br ov m, 14H, C*H*$_2$), 1.12 (d, $^3J_{HH}$ = 6.7 Hz, 12H, C*H*$_3$), 0.50 (d, $^2J_{HP}$ = 62.9 Hz, 2H, Sc–C*H*). ^{13}C{^{1}H} NMR (benzene-d_6): 148.3 (d, J_{CP} = 6.3 Hz, aromatic *ipso*-C), 138.3 (s, aromatic *ipso*-C), 128.0 (s, aromatic *ipso*-C), 127.7 (s, aromatic *ipso*-C), 127.1 (s, aromatic CH), 124.3 (s, aromatic CH), 124.23 (s, aromatic *ipso*-C), 124.20 (s, aromatic CH), 120.5 (d, J_{CP} = 15.8 Hz, aromatic CH), 114.9 (d, J_{CP} = 70.2 Hz, aromatic *ipso*-C), 33.5 (s, CH(CH$_3$)$_2$), 32.2 (br m, Sc–CH), 32.2 (d, $^2J_{CP}$ = 3.8 Hz, P–CH$_2$CH$_2$), 30.2 (d, $^2J_{CP}$ = 17.4 Hz, P–CH$_2$CH$_2$), 24.3 (s, CH(CH$_3$)$_2$), 21.6 (s, Ar–CH$_3$), 21.5 (d, $^1J_{CP}$ = 43.8 Hz, P–CH$_2$). ^{31}P{^{1}H} NMR (benzene-d_6): δ 56.2. In situ formation and thermal instability of complex **15** rendered isolation of analytically pure samples for EA analysis impossible. Therefore, these data were not obtained.

X-ray crystallography

Recrystallization of compound **3** from toluene, **4** and **9** from pentane, and **5** and **10** from benzene layered with pentane afforded single crystals suitable for X-ray diffraction. Crystals were coated in hydrocarbon oil under an argon atmosphere and mounted onto a glass fibre. Data were collected at –100 °C using a Bruker SMART APEX II diffractometer (Mo Kα radiation, λ = 0.71 073 Å) outfitted with a CCD area-detector and a KRYOFLEX liquid nitrogen vapour cooling device. A data collection strategy using ω and φ scans at 0.5° steps yielded full hemispherical data with excellent intensity statistics. Unit cell parameters were determined and refined on all observed reflections using APEX2 software.[18] Data reduction and correction for Lorentz polarization were performed using SAINT-Plus software.[19] Absorption corrections were applied using SADABS.[20] The structures were solved by direct methods and refined by the least squares method on F^2 using the SHELXTL software suite.[21] All non-hydrogen atoms were refined anisotropically, except in certain cases of disorder (vide infra). Hydrogen atom positions were calculated and isotropically refined as riding models to their parent atoms. Table 7 provides a summary of selected data collection and refinement parameters. Special considerations were required in the refinement of disordered moieties in the structure of **5**, where one *para*-isopropylphenyl group (C28, 52%/C28b, 48%) was disordered. Disordered atoms were refined as isotropic mixtures and some restraints were applied to obtain reasonable bond distances and angles.

Supplementary data

Supplementary data are available with the article through the journal Web site at http://nrcresearchpress.com/doi/suppl/10.1139/cjc-2015-0368.

CCDC 1429584 (**3**), 1429585 (**4**), 1429586 (**5**), 1429587 (**9**), and 1429588 (**10**) contain the supplementary crystallographic data for this paper. These data can be obtained, free of charge, via http://www.ccdc.cam.ac.uk/products/csd/request/ or from the Cambridge Crystallographic Data Centre, 12 Union Road, Cambridge CB2 1EZ UK; fax: 44-1223-336033 or e-mail: deposit@ccdc.cam.ac.uk.

Acknowledgements

This research was financially supported by the Natural Sciences and Engineering Research Council of Canada and the Canada Foundation for Innovation (CFI).

References

(1) Johnson, K. R. D.; Hayes, P. G. *Chem. Soc. Rev.* **2013**, *42*, 1947. doi:10.1039/c2cs35356c.

(2) (a) Johnson, K. R. D.; Hayes, P. G. *Organometallics* **2009**, *28*, 6352. doi:10.1021/om900731x; (b) Johnson, K. R. D.; Hayes, P. G. *Organometallics* **2013**, *32*, 4046. doi:10.1021/om400413e; (c) Johnson, K. R. D.; Hayes, P. G. *Dalton Trans.* **2014**, *43*, 2448. doi:10.1039/C3DT52790E; (d) Johnson, K. R. D.; Hayes, P. G. *Inorg. Chim. Acta* **2014**, *422*, 209. doi:10.1016/j.ica.2014.05.045.

(3) Johnson, K. R. D.; Hayes, P. G. *Organometallics* **2011**, *30*, 58. doi:10.1021/om100814h.

(4) Masuda, J. D.; Jantunen, K. C.; Scott, B. L.; Kiplinger, J. L. *Organometallics* **2008**, *27*, 1299. doi:10.1021/om701159d.

(5) Lukešová, L.; Ward, B. D.; Bellemin-Laponnaz, S.; Wadepohl, H.; Gade, L. H. *Organometallics* **2007**, *26*, 4652. doi:10.1021/om700504f.

(6) Arndt, S.; Zeimentz, P. M.; Spaniol, T. P.; Okuda, J.; Honda, M.; Tatsumi, K. *Dalton Trans.* **2003**, 3622. doi:10.1039/B305964B.

(7) Lu, E.; Li, Y.; Chen, Y. *Chem. Commun.* **2010**, *46*, 4469. doi:10.1039/c002870c.

(8) Conroy, K. D.; Piers, W. E.; Parvez, M. *J. Organomet. Chem.* **2008**, *693*, 834. doi:10.1016/j.jorganchem.2007.08.037.

(9) Rufanov, K. A.; Spannenberg, A. *Mendeleev Commun.* **2008**, *18*, 32. doi:10.1016/j.mencom.2008.01.013.

(10) Hacklin, H.; Röschenthaler, G.-V. *Phosphorus Sulfur Relat. Elem.* **1988**, *36*, 165. doi:10.1080/03086648808079013.

(11) (a) Johnson, K. R. D.; Hannon, M. A.; Ritch, J. S.; Hayes, P. G. *Dalton Trans.* **2012**, *41*, 7873. doi:10.1039/C2DT12485H; (b) Zamora, M. T.; Johnson, K. R. D.; Hänninen, M. M.; Hayes, P. G. *Dalton Trans.* **2014**, *43*, 10739. doi:10.1039/C4DT00863D.

(12) Zeimentz, P. M.; Okuda, J. *Organometallics* **2007**, *26*, 6388. doi:10.1021/om7007953.

(13) Watson, P. L. *J. Chem. Soc., Chem. Commun.* **1983**, 276. doi:10.1039/C39830000276.

(14) Wayda, A. L.; Atwood, J. L.; Hunter, W. E. *Organometallics* **1984**, *3*, 939. doi:10.1021/om00084a023.

(15) (a) Konkol, M.; Kondracka, M.; Voth, P.; Spaniol, T. P.; Okuda, J. *Organometallics* **2008**, *27*, 3774. doi:10.1021/om800161u; (b) Bambirra, S.; Brandsma, M. J. R.; Brussee, E. A. C.; Meetsma, A.; Hessen, B.; Teuben, J. H. *Organometallics* **2000**, *19*, 3197. doi:10.1021/om0001063; (c) Mitchell, J. P.; Hajela, S.; Brookhart, S. K.; Hardcastle, K. I.; Henling, L. M.; Bercaw, J. E. *J. Am. Chem. Soc.* **1996**, *118*, 1045. doi:10.1021/ja953419b.

(16) (a) Schumann, H.; Freckmann, D. M. M.; Dechert, S. *Z. Anorg. Allg. Chem.* **2002**, *628*, 2422. doi:10.1002/1521-3749(200211)628:11<2422::AID-ZAAC2422>3.0.CO;2-B; (b) Masuda, J. D.; Jantunen, K. C.; Ozerov, O. V.; Noonan, K. J. T.; Gates, D. P.; Scott, B. L.; Kiplinger, J. L. *J. Am. Chem. Soc.* **2008**, *130*, 2408. doi:10.1021/ja7105306; (c) Estler, F.; Eickerling, G.; Herdtweck, E.; Anwander, R. *Organometallics* **2003**, *22*, 1212. doi:10.1021/om020783s; (d) Arndt, S.; Voth, P.; Spaniol, T. P.; Okuda, J. *Organometallics* **2000**, *19*, 4690. doi:10.1021/om000506q.

(17) Lappert, M. F.; Pearce, R. *J. Chem. Soc. Chem. Commun.* **1973**, 126. doi:10.1039/C39730000126.

(18) *APEX2*, 2010.7-0; Bruker AXS: Madison, WI, 2010.

(19) *SAINT-Plus*, 7.68A; Bruker AXS: Madison, WI, 2009.

(20) Sheldrick, G. M. *SADABS*, 2008/1; Bruker AXS: Madison, WI, 2008.

(21) Sheldrick, G. M. *Acta Crystallogr. Sect. A: Found. Crystallogr.* **2007**, *64*, 112. doi:10.1107/S0108767307043930.

Can. J. Chem. Downloaded from www.nrcresearchpress.com by University of Lethbridge on 04/11/16
For personal use only.